

# Spatial distributions of particle number concentrations in the global troposphere: Simulations, observations, and implications for nucleation mechanisms

Fangqun Yu,<sup>1</sup> Gan Luo,<sup>1</sup> Timothy S. Bates,<sup>2</sup> Bruce Anderson,<sup>3</sup> Antony Clarke,<sup>4</sup> Vladimir Kapustin,<sup>4</sup> Robert M. Yantosca,<sup>5</sup> Yuxuan Wang,<sup>6</sup> and Shiliang Wu<sup>7</sup>

Received 1 November 2009; revised 16 April 2010; accepted 5 May 2010; published 9 September 2010.

[1] Particle number concentration in the troposphere is an important parameter controlling the climate and health impacts of atmospheric aerosols. We show that nucleation rates and total particle number concentrations in the troposphere, predicted by different nucleation schemes, differ significantly. Our extensive comparisons of simulated results with land-, ship-, and aircraft-based measurements indicate that, among six widely used nucleation schemes involving sulfuric acid, only the ion-mediated nucleation (IMN) scheme can reasonably account for both absolute values (within a factor of  $\sim 2$ ) and spatial distributions of particle number concentrations in the whole troposphere. Binary homogeneous nucleation (BHN) schemes significantly underpredict particle number concentration in the lower troposphere (below  $\sim 500$  mbar), especially in the boundary layer over major continents (by a factor of up to  $\sim 10$ ). BHN is also insignificant in the upper troposphere based on a recent kinetically self-consistent nucleation model constrained by multiple independent laboratory data. Previous conclusions about the importance of BHN in the upper troposphere should be revisited. Empirical activation and kinetic nucleation formulas significantly overpredict the particle number concentrations over tropical and subtropical oceans (by a factor of up to  $\sim 10$  in the boundary layer), and the overpredictions extend from ocean surface to around  $\sim 400$  mbar. This study represents the first comprehensive comparison of global particle number simulations with relevant measurements that have a 3-D global spatial coverage. Our results suggest that ion-mediated  $\text{H}_2\text{SO}_4\text{-H}_2\text{O}$  nucleation appears to dominate over neutral  $\text{H}_2\text{SO}_4\text{-H}_2\text{O}$  nucleation, not only in the lower troposphere but also in the middle and upper troposphere.

**Citation:** Yu, F., G. Luo, T. S. Bates, B. Anderson, A. Clarke, V. Kapustin, R. M. Yantosca, Y. Wang, and S. Wu (2010), Spatial distributions of particle number concentrations in the global troposphere: Simulations, observations, and implications for nucleation mechanisms, *J. Geophys. Res.*, 115, D17205, doi:10.1029/2009JD013473.

## 1. Introduction

[2] Aerosol particles appear in the troposphere because of either in situ nucleation (i.e., secondary particles) or direct

emissions (i.e., primary particles). In addition to the mass concentration, the particle number concentration affects the climate and health impacts of atmospheric aerosols. Field measurements show clearly that the number concentrations of cloud drops increase with increasing total aerosol number concentrations [e.g., Ramanathan *et al.*, 2001]. High number concentrations of ultrafine particles may also lead to adverse health effects [e.g., Penttinen *et al.*, 2001; Oberdörster *et al.*, 2004].

[3] Because of the importance of knowing accurately the aerosol number concentrations and their spatiotemporal variations, more and more global models are beginning to include explicit calculations of the new particle formation and size-resolved aerosol microphysics [e.g., Bauer *et al.*, 2008; Spracklen *et al.*, 2008; Makkonen *et al.*, 2009; Wang and Penner, 2009; Pierce and Adams, 2009; Yu and Luo, 2009]. Nucleation, which has been frequently observed in many parts of the troposphere [e.g., Clarke and Kapustin, 2002; Kulmala *et al.*, 2004; Yu *et al.*, 2008], is an important

<sup>1</sup>Atmospheric Sciences Research Center, State University of New York at Albany, Albany, New York, USA.

<sup>2</sup>Pacific Marine Environmental Laboratory, National Oceanic and Atmospheric Administration, Seattle, Washington, USA.

<sup>3</sup>Chemistry and Dynamics Branch, Science Directorate, NASA Langley Research Center, Hampton, Virginia, USA.

<sup>4</sup>Department of Oceanography, University of Hawai'i at Mānoa, Honolulu, Hawaii, USA.

<sup>5</sup>School of Engineering and Applied Sciences, Harvard University, Cambridge, Massachusetts, USA.

<sup>6</sup>Department of Environmental Science and Engineering, Tsinghua University, Beijing, China.

<sup>7</sup>Department of Geological and Mining Engineering and Sciences and Department of Civil and Environmental Engineering, Michigan Technological University, Houghton, Michigan, USA.

**Table 1.** Six Nucleation Schemes and Corresponding Variables Controlling the Predicted Nucleation Rates (J)<sup>a</sup>

Nucleation Model/Parameterization	Controlling Variables	References
Ion-mediated nucleation (IMN)	$J_{\text{IMN}} = f([\text{H}_2\text{SO}_4], T, \text{RH}, Q, S)$	<i>Yu and Turco</i> [2000]; <i>Yu</i> [2006b, 2010].
Ion-induced nucleation (IIN)	$J_{\text{IIN}} = f([\text{H}_2\text{SO}_4], T, \text{RH}, Q, S)$	<i>Lovejoy et al.</i> [2004]; <i>Modgil et al.</i> [2005]
Kinetic binary homogeneous nucleation (KBHN)	$J_{\text{KBHN}} = f([\text{H}_2\text{SO}_4], T, \text{RH})$	<i>Yu</i> [2007, 2008]
Classical binary homogeneous nucleation (CBHN)	$J_{\text{CBHN}} = f([\text{H}_2\text{SO}_4], T, \text{RH})$	<i>Noppel et al.</i> [2002]; <i>Vehkamäki et al.</i> [2002]
Empirical activation nucleation (EAN)	$J_{\text{EAN}} = A [\text{H}_2\text{SO}_4]$ , $A = 3.5 \times 10^{-7}$ used in this study	<i>Riipinen et al.</i> [2007]; <i>Kuang et al.</i> [2008]
Empirical kinetic nucleation (EKN)	$J_{\text{EKN}} = K [\text{H}_2\text{SO}_4]^2$ , $K = 5.5 \times 10^{-14}$ used in this study	<i>Riipinen et al.</i> [2007]; <i>Kuang et al.</i> [2008]

<sup>a</sup>Nucleation schemes IMN, IIN, KBHN, CBHN, EAN, and EKN are used in the present study.  $J_{\text{IMN}}$  and  $J_{\text{IIN}}$  depend on sulfuric acid vapor concentration ( $[\text{H}_2\text{SO}_4]$ ), temperature (T), relative humidity (RH), ionization rate (Q), and surface area of preexisting particles (S).  $J_{\text{KBHN}}$  and  $J_{\text{CBHN}}$  depend on  $[\text{H}_2\text{SO}_4]$ , T, and RH.  $J_{\text{EAN}}$  and  $J_{\text{EKN}}$  depend on  $[\text{H}_2\text{SO}_4]$  only.

source of global particles and appears to dominate the total particle number abundance in most parts of the troposphere [Yu and Luo, 2009]. While in situ measurements have long established the involvement of sulfuric acid gas in atmospheric nucleation [e.g., Weber et al., 1996; Clarke et al., 1998], a consensus in the scientific community with regard to the dominant nucleation mechanism(s) remains to be achieved despite decades of investigation on atmospheric nucleation phenomena. Nucleation theories of various kinds and versions have been continuously developed and updated by different research groups. As a result of the uncertainties in the thermodynamic data and various approximations employed in theoretical derivations, the nucleation rates predicted by different nucleation theories/parameterizations differ by many orders of magnitude [Yu and Turco, 2008]. More importantly, different kinds of nucleation theories have different sensitivities to key parameters. A recent global simulation indicates that aerosol indirect forcing is sensitive to the nucleation process [Wang and Penner, 2009]. In order to assess the aerosol indirect radiative forcing and confidently project the future climate change, identification of the dominant particle formation mechanism (s) and key controlling parameters is imperative.

[4] In this study, we employ a recently developed global size-resolved aerosol microphysics model [Yu and Luo, 2009] to study the difference in the number concentrations of atmospheric aerosols and their spatial distributions predicted by different nucleation schemes. The modeling results are compared with an extensive set of land-, ship-, and aircraft-based measurements, aiming to assess the ability of different nucleation theories in capturing the spatial distributions of global particle number concentrations and to identify the nucleation scheme(s) that can reasonably account for the observations.

## 2. Overview of Nucleation Theories/Schemes and Their Differences

[5] There exist three relatively well-developed atmospheric nucleation theories: (1) binary homogeneous nucleation (BHN) of  $\text{H}_2\text{SO}_4$  and  $\text{H}_2\text{O}$  [e.g., Noppel et al., 2002; Vehkamäki et al., 2002; Yu, 2007, 2008], (2) ternary homogeneous nucleation (THN) of  $\text{H}_2\text{SO}_4$ - $\text{H}_2\text{O}$ - $\text{NH}_3$  [e.g., Napari et al., 2002; Yu, 2006a; Merikanto et al., 2007], and (3) ion-mediated nucleation (IMN) [Yu and Turco, 2000; Yu, 2006b, 2010] or ion-induced nucleation (IIN) [e.g., Lovejoy et al., 2004; Sorokin et al., 2006] of  $\text{H}_2\text{SO}_4$ - $\text{H}_2\text{O}$ -Ion. In addition, a number of regression analyses indicate

that the particle formation rates derived from observations have a linear or square dependence on  $\text{H}_2\text{SO}_4$  vapor concentration ( $[\text{H}_2\text{SO}_4]$ ) [e.g., Riipinen et al., 2007; Kuang et al., 2008], and empirical activation and kinetic nucleation formulas have been used in several studies to represent boundary layer nucleation. On the basis of the kinetic THN model constrained by laboratory studies [Yu, 2006a] and the revised classical THN model [Merikanto et al., 2007], THN is likely to be negligible in both the boundary layer because of high temperature [Yu and Turco, 2008] and the upper troposphere because of lower ammonia concentration. In the present study, we focus on binary homogeneous, ion, and empirical nucleation, with two different schemes selected for each category. Details of these nucleation schemes are given in Table 1. These six nucleation schemes represent the most recently updated version of corresponding nucleation schemes currently available from several research groups.

[6] Figure 1 shows the predicted nucleation rates based on six different nucleation schemes ( $J_X$ ,  $X = \text{IMN, IIN, KBHN, CBHN, EAN, EKN}$ ; see Table 1) as a function of  $[\text{H}_2\text{SO}_4]$ , temperature (T), relative humidity (RH), and surface area of preexisting particles (S). Nucleation rates under the same conditions given by two different parameterizations of the same nucleation kind differ by up to many orders of magnitude.  $J_{\text{IMN}}$  is generally several orders of magnitude higher than  $J_{\text{IIN}}$ . The possible cause of the difference has been discussed in Yu [2006b] and Yu and Turco [2008]. It should be noted that an increase in  $J_{\text{IIN}}$  as T increases when  $T > 290$  K (Figure 1d) and as  $[\text{H}_2\text{SO}_4]$  decreases when  $[\text{H}_2\text{SO}_4] < \sim 2 \times 10^6 \text{ cm}^{-3}$  (Figure 1b) is physically unrealistic and likely to be caused by the error in the parameterization of Modgil et al. [2005]. Thus, care must be taken in using the parameterization of Modgil et al. [2005] in regional and global simulations as it may give erroneously high nucleation rates when  $T > \sim 290$  K and  $[\text{H}_2\text{SO}_4] < \sim 10^6 \text{ cm}^{-3}$ . In the present study,  $J_{\text{IIN}}$  is set to zero when  $T > 290$  K, or when  $[\text{H}_2\text{SO}_4] < 10^6 \text{ cm}^{-3}$  if  $290 \text{ K} > T > 270 \text{ K}$ . The application of this filter will not affect results because under such conditions, nucleation rate is generally negligible even based on IMN. The BHN is negligible in the warm lower troposphere but could be significant in the cold upper troposphere. At colder T,  $J_{\text{CBHN}}$  is several orders of magnitude higher than  $J_{\text{KBHN}}$ . Laboratory studies [Hanson and Lovejoy, 2006] have shown that the Vehkamäki et al. [2002] model overpredicted the BHN rates by about three orders of magnitude at low T. A significant overprediction may mislead one to think that BHN can account for the observed new particle formation rates in the upper troposphere while in reality the observed

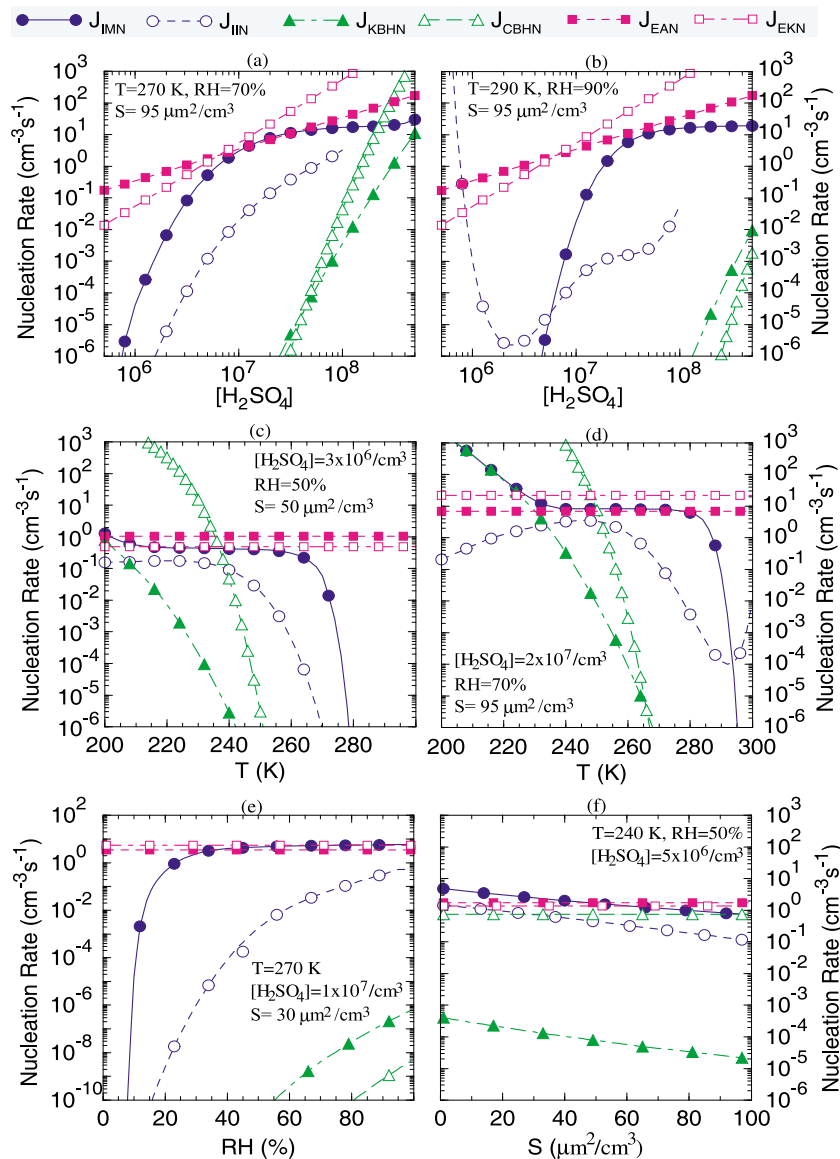


**Figure 1.** The dependence of nucleation rates on (a, b)  $[\text{H}_2\text{SO}_4]$ , (c, d)  $T$ , (e)  $\text{RH}$ , and (f)  $S$ , based on six nucleation schemes described in Table 1 under selected conditions. Ionization rate ( $Q$ ) is assumed to be  $10$  ion-pairs  $\text{cm}^{-3}\text{s}^{-1}$  for all IMN and IIN cases, and the values of other parameters are specified in the legend.

nucleation events might be dominated by other mechanisms. The kinetic binary homogeneous nucleation (KBHN) model [Yu, 2007, 2008], which is constrained by multiple independent laboratory data sets (including those of *Hanson and Lovejoy* [2006]), appears to be more accurate.  $J_{\text{EAN}}$  and  $J_{\text{EKN}}$  with the assumed values of prefactors  $A$  and  $K$  are generally higher than  $J_{\text{IMN}}$ , especially at high  $T$ . Prefactors  $A$  and  $K$ , derived from different measurements, vary by up to approximately four orders of magnitude [Riipinen et al., 2007; Kuang et al., 2008]. It remains to be studied what controls the variations of  $A$  and  $K$ . In the present study, the mean values of  $A$  and  $K$  derived from Hyttiälä measurements [Riipinen et al., 2007] are assumed.

[7]  $[\text{H}_2\text{SO}_4]$  and  $T$  appear to be the two most important parameters controlling the formation rates of particles in the troposphere [Yu, 2010]. It is clear from Figure 1 that the

dependence of  $J$  on  $[\text{H}_2\text{SO}_4]$  and  $T$  differs significantly, with important implications for how future climate and emission changes may impact new particle formation, aerosol indirect radiative forcing, and climate feedback mechanisms [Yu, 2010]. Compared to  $J_{\text{IMN}}$ ,  $J_{\text{CBHN}}$  and  $J_{\text{KBHN}}$  are generally more sensitive to the changes in  $T$  and  $[\text{H}_2\text{SO}_4]$ . Under the conditions shown in Figure 1e,  $J_{\text{IMN}}$  is very sensitive to  $\text{RH}$  when  $\text{RH}$  is low ( $< \sim 20\%$ ), but the sensitivity decreases as  $\text{RH}$  increases.  $J_{\text{EAN}}$  and  $J_{\text{EKN}}$  have a weaker dependence on  $[\text{H}_2\text{SO}_4]$  and no dependence on  $T$ ,  $\text{RH}$ , and  $S$ . It is interesting to note that  $J_{\text{IMN}}$  and  $J_{\text{EAN}}$ , within certain parameter spaces, are close in terms of absolute values and their sensitivities to  $[\text{H}_2\text{SO}_4]$ ,  $T$ , and  $\text{RH}$ . The dependence of  $J_{\text{IMN}}$  on  $T$ ,  $[\text{H}_2\text{SO}_4]$ , and  $\text{RH}$  is nonlinear because of limitations in other parameters, especially ionization rates. Future climate and emission changes are expected to substantially change  $T$

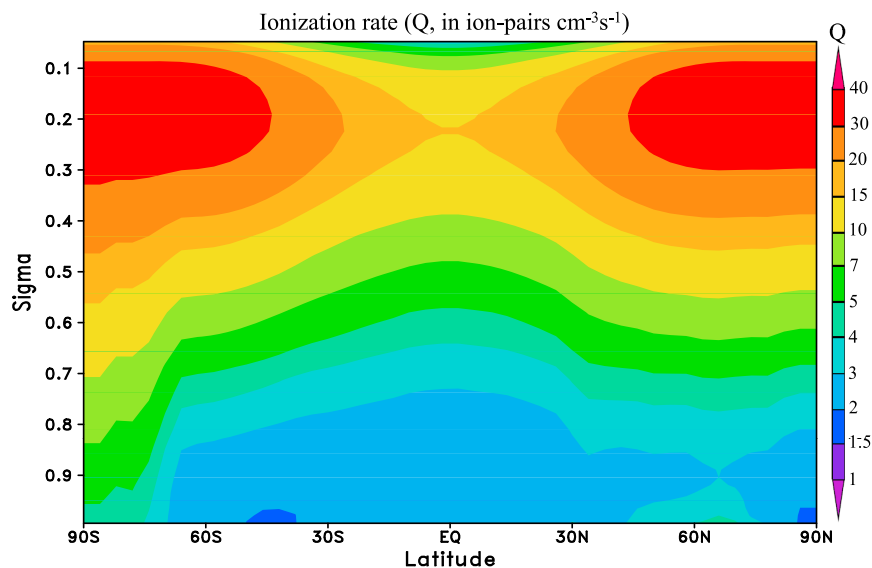


**Figure 2.** Vertical (sigma equals pressure divided by surface pressure) structure of annual mean, zonally averaged ionization rates due to galactic cosmic rays and radioactive materials from soil.

and  $[\text{H}_2\text{SO}_4]$  in different parts of the atmosphere, and different nucleation theories may predict quite different nucleation rates, which would impact aerosol indirect radiative forcing and thus climate feedback processes. In addition, ionization rate variations associated with solar activities will affect the ion nucleation rates [Yu, 2010], but will have no influence on neutral nucleation. Therefore, it is critically important to identify the dominant nucleation mechanism(s) in the atmosphere.

[8] Because of large spatial and temporal variations of  $T$ ,  $[\text{H}_2\text{SO}_4]$ , and other parameters in the atmosphere, nucleation rates and total particle number concentrations in the global troposphere predicted by different nucleation schemes are expected to differ significantly. With a global aerosol microphysics model, different nucleation schemes for new particle formation can be evaluated quantitatively by comparing the predicted particle number concentrations with the field data taken in different parts of the atmosphere during the past two decades.

### 3. Global Size-Resolved Aerosol Microphysics Model

[9] GEOS-Chem, a global 3-D model of atmospheric composition driven by assimilated meteorological data from the NASA Goddard Earth Observing System 5 (GEOS-5), is employed for this study. The GEOS-Chem model has been developed and used by research groups worldwide and contains many state-of-the-art modules treating various chemical and aerosol processes [e.g., Bey et al., 2001; Martin et al., 2003; Park et al., 2004; Evans and Jacob, 2005; Nenes et al., 1998; Liao et al., 2007] with up-to-date key emission inventories [e.g., Bond et al., 2007; Zhang et al., 2009]. A detailed description of the model (including the treatment of various emission sources, chemistry, and aerosol schemes) can be found in the model Web site (<http://acmg.seas.harvard.edu/geos>).

[10] Recently, Yu and Luo [2009] incorporated an advanced particle microphysics (APM) model into GEOS-Chem to treat size-resolved microphysics, dry deposition, and wet scavenging for aerosols. In the present version of the aerosol module, size-resolved microphysics for secondary particles (i.e., those formed from gaseous species) and sea salt has been treated with 40 sectional bins to represent sulfate (or secondary) particles and 20 sectional bins to represent sea salt particles. The bin structure is chosen to have relatively high resolution for the size range important to the growth of nucleated particles (a few nanometers) to cloud condensation nuclei. The growth of nucleated particles through the condensation of sulfuric acid vapor and equilibrium uptake of nitrate, ammonium, and secondary organic aerosol is explicitly simulated, along with the scavenging of secondary particles by primary particles (dust, black carbon, organic carbon, and sea salt). More details of the aerosol model can be found in Yu and Luo [2009]. The APM module, after some further improvement and proper validation, will be added to the standard version of GEOS-Chem in the near future.

[11] Here, we extend the studies presented in Yu and Luo [2009] by simulating the same period (year 2006) based on the six different nucleation schemes given in Table 1, with a horizontal resolution of  $4^\circ \times 5^\circ$  and 47 vertical layers up to 0.01 hPa (GEOS-5 meteorological fields). GEOS-Chem v8-01-03 used in Yu and Luo [2009] has been updated to v8-02-02 for the present simulation. To clearly compare the differences, the fraction of anthropogenic sulfur emitted as primary sulfate (used to represent the subgrid nucleation process) has been set to zero. The oceanic  $\alpha$ -pinene emission indicated by ship measurements is not considered in the present study because of the large unresolved difference between the total fluxes derived from “top-down” and “bottom-up” approaches [Luo and Yu, 2010]. The global ionization rates due to cosmic rays are calculated on the basis of the schemes given in Usoskin and Kovaltsov [2006] and the contribution of radioactive materials from soil to

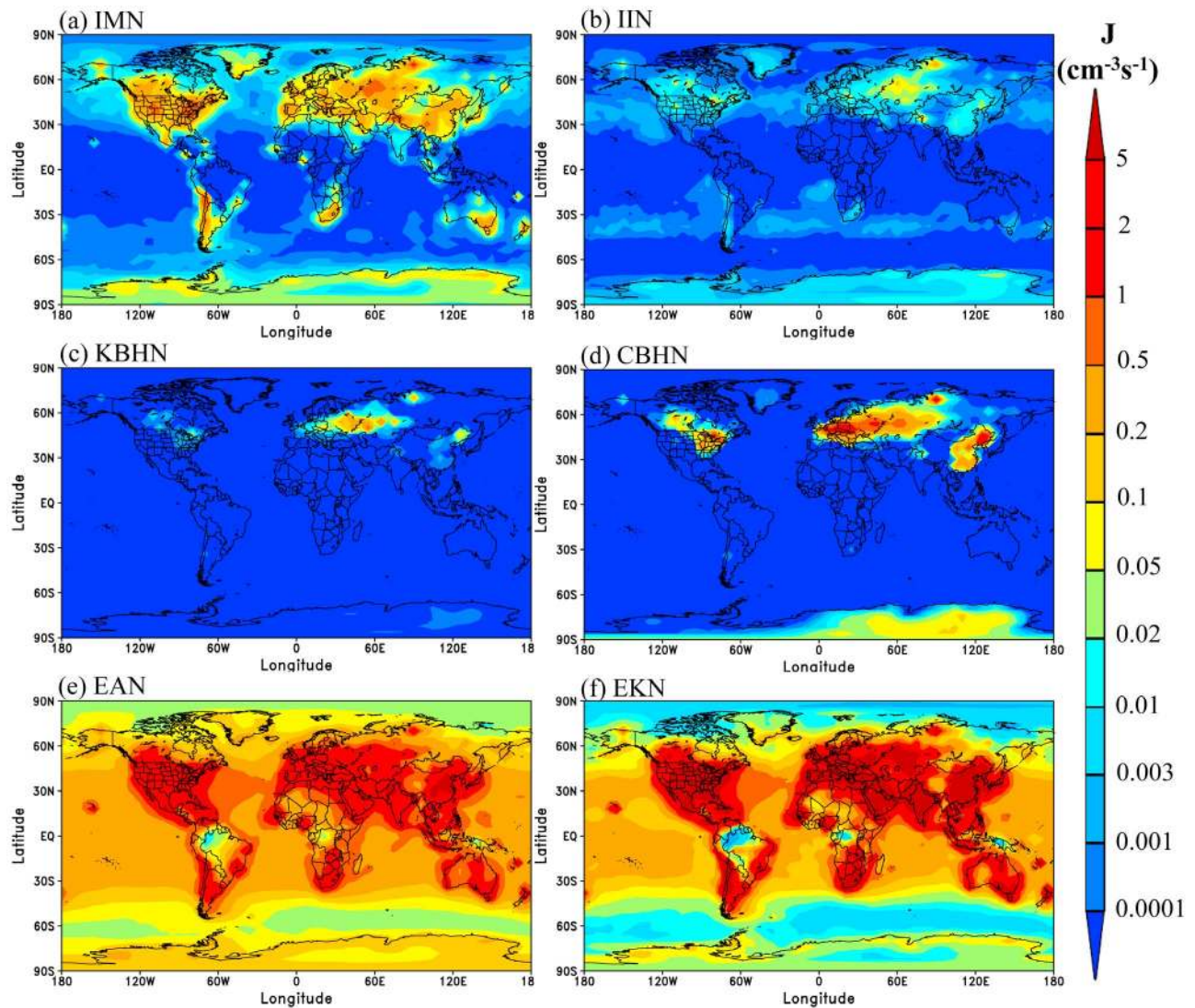


**Figure 3.** Horizontal spatial distributions of annual mean nucleation rates in the lower boundary layer (0–0.4 km) simulated with six different nucleation schemes described in Table 1.

ionization rates is parameterized on the basis of the profiles given in Reiter [1992]. Figure 2 gives the calculated zonally averaged annual mean ionization rates ( $Q$ , in ion-pairs  $\text{cm}^{-3}\text{s}^{-1}$ ). In the lower troposphere,  $Q$  is generally below  $10$  ion-pairs  $\text{cm}^{-3}\text{s}^{-1}$ . In the upper troposphere,  $Q$  is in the range of  $10$ – $20$  ion-pairs  $\text{cm}^{-3}\text{s}^{-1}$  at the low latitudes ( $30^\circ\text{S}$  to  $30^\circ\text{N}$ ) and  $20$ – $40$  ion-pairs  $\text{cm}^{-3}\text{s}^{-1}$  at the high latitudes.

#### 4. Global Simulations and Comparisons With Measurements

[12] Figures 3 and 4 present the horizontal (averaged within lower boundary layer 0–0.4 km, annual mean) and vertical (zonal-averaged, annual mean) spatial distributions of nucleation rates based on the six different nucleation schemes described in Table 1. As expected, nucleation rates predicted on the basis of different schemes vary significantly both in absolute values and in their spatial distributions. Throughout the troposphere, the annual mean  $J_{\text{IIN}}$  is a factor of  $\sim 10$ – $100$  smaller than  $J_{\text{IMN}}$ , while  $J_{\text{KBHN}}$  is a factor of

$\sim 10$ – $100$  lower than  $J_{\text{CBHN}}$ . Classical binary homogeneous nucleation (CBHN) theory predicts largest nucleation rates in the upper troposphere. CBHN theory also predicts large nucleation rates in polar upper troposphere, differing substantially from predictions based on other nucleation schemes. Large differences in annual mean nucleation rates predicted on the basis of the ion nucleation and BHN models have significant implications with regard to the relative importance of ion versus neutral nucleation as a source of new particles in the troposphere. On the basis of CBHN, neutral binary homogeneous nucleation dominates over ion nucleation in the upper troposphere. However, on the basis of KBHN, ion nucleation (IMN or IIN) dominates throughout the troposphere. BHN has long been suggested as a major source of new particles in the upper troposphere. As we have pointed out in section 2, the KBHN model is consistent with recent laboratory data and its predictions should be considered more robust than CBHN. Therefore, it is reasonable to conclude that ion nucleation dominates neutral nucleation, not only in the lower troposphere but

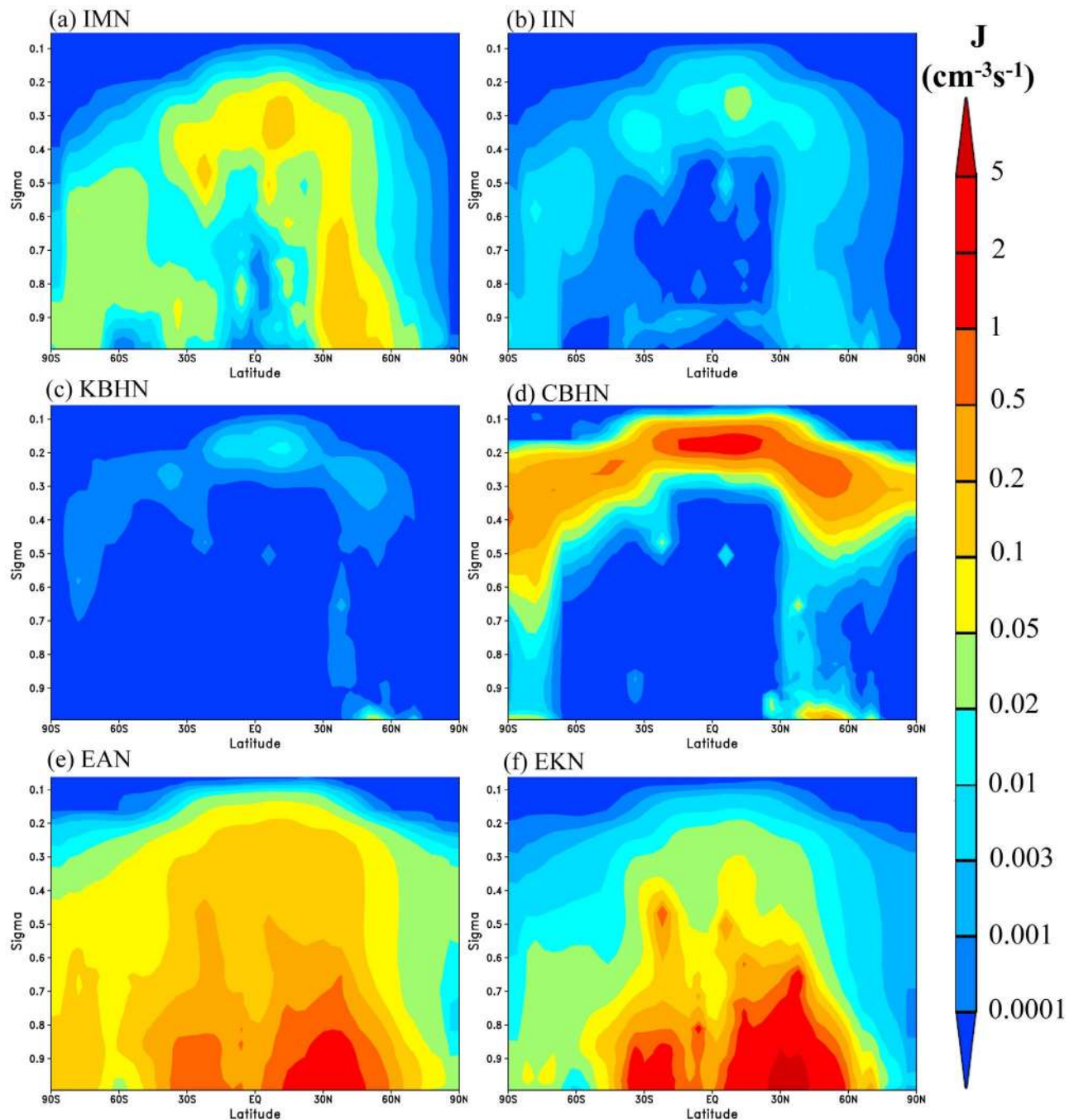


**Figure 4.** Vertical (sigma equals pressure divided by surface pressure) structure of annual mean, zonally averaged nucleation rates predicted with six different nucleation schemes described in Table 1.

also in the middle and upper troposphere. This appears to be physically sound since ions are known to enhance the nucleation as a result of charge effects on cluster stability and growth rates [Yu, 2010]. There is no physical reason that the homogeneous nucleation rate exceeds ion nucleation rates except under the conditions when the nucleation rate is larger than the ionization rate (i.e., when  $J_{\text{IMN}}$  is limited by ionization rate; see Figure 1). Our simulations indicate that the conditions in the ambient troposphere generally do not reach the level that nucleation rates (Figures 3 and 4) exceed ion production rates (Figure 2).

[13] Both empirical activation nucleation (EAN) and empirical kinetic nucleation (EKN) predict very large nucleation rates in most parts of the troposphere and give nucleation rates spatial distributions quite different from those based on ion and neutral nucleation theories. The empirical formulas (EAN and EKN) predict widespread nucleation over tropical and subtropical oceans, in dramatic contrast to those based on theoretical models (IMN, IIN, KBHN, and CBHN). The main reason is the effect of temperature, which is not considered in empirical formulas. Another significant difference is that theoretical models

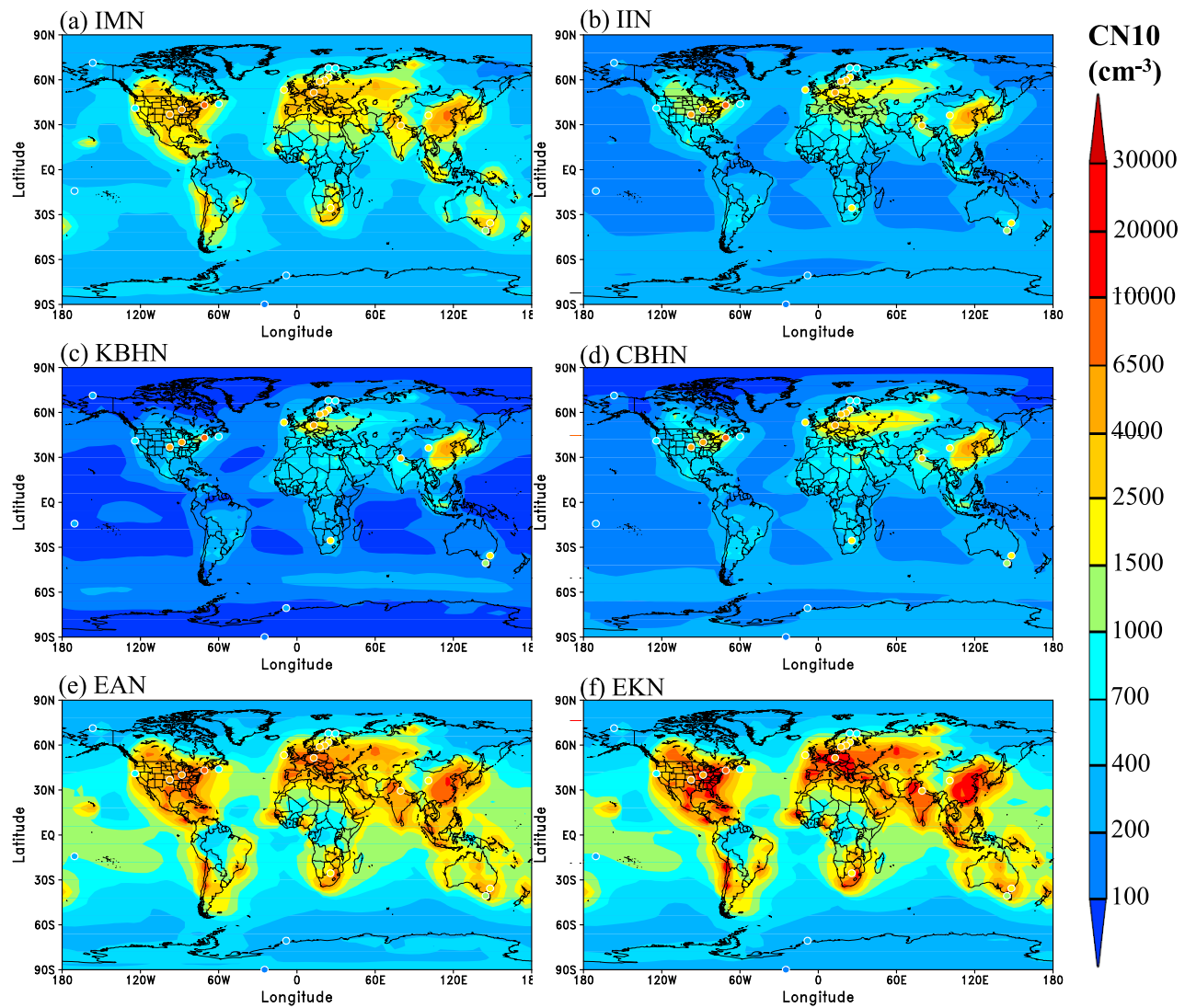


**Figure 5.** Horizontal distributions of annual mean number concentrations of condensation nuclei larger than 10 nm (CN10) in the lower boundary layer (0–0.4 km) simulated with six different nucleation schemes described in Table 1. The observed annual or multiple year averaged CN10 values from 21 sites are also overlapped on the plots for comparison.

predict a high nucleation rate zone in the tropical upper troposphere while empirical formulas do not predict such a zone. The reason again is associated with the effect of temperature.  $[\text{H}_2\text{SO}_4]$  generally decreases with altitude, and this is why  $J_{\text{EAN}}$  and  $J_{\text{EKN}}$  decrease with altitude. The theoretical models give a higher nucleation rate in the upper troposphere because of the lower  $T$  which favors the nucleation based on the nucleation thermodynamics.

[14] In the last two decades, particle number concentrations have been measured in different parts of troposphere with land-, ship-, and aircraft-based instruments. A number of surface-based stations have long-term (multiple-year) continuous measurements of total number concentration of particles larger than  $\sim 10$  nm (CN10). The ship- and aircraft-based measurements of particle number concentrations have limitations in the duration of the observations, but provide a much wider spatial coverage, which is necessary for global 3-D comparisons. The particle number concentration data

from these measurement campaigns and monitoring stations can be used to assess the ability of various nucleation schemes to capture the absolute values as well as the spatial distributions of particle number concentrations.

[15] Figure 5 shows the horizontal spatial distributions of annual mean number concentrations of CN10 averaged within the lower boundary layer (0–0.4 km), simulated with the six nucleation schemes described in Table 1. Overlaid on each panel for comparison (symbols) are the 19 observed annual or multiple-year averaged CN10 values compiled in *Yu and Luo* [2009] plus two additional data points from recent literature:  $2730 \text{ cm}^{-3}$  in Mukteshwar, India [*Komppula et al.*, 2009], and  $2030 \text{ cm}^{-3}$  in Mount Waliguan, China [*Kivekäs et al.*, 2009]. A more specific comparison of simulated CN10 with observed values is presented in Figure 6 where the simulated values based on different nucleation schemes are plotted against corresponding observed values. It is clear from Figures 5 and 6 that, under the present model

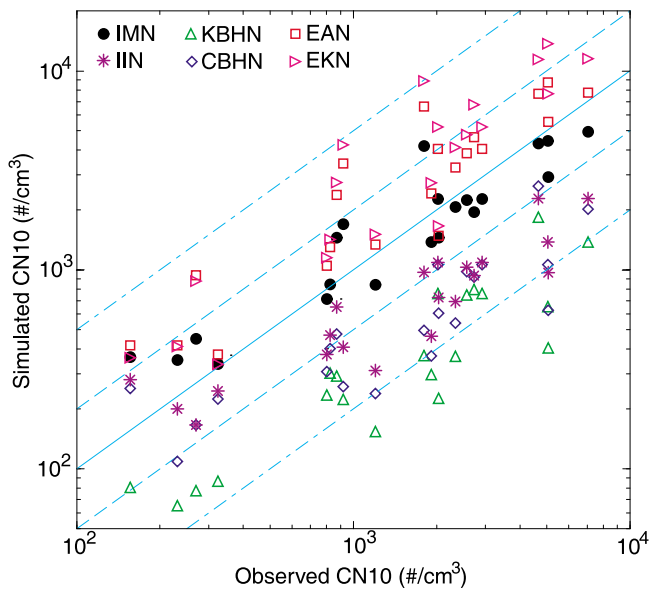


Figure 6

**Figure 6.** Comparison of annually averaged number concentrations of CN10 observed at 21 sites shown in Figure 5 with those simulated on the basis of six different nucleation schemes described in Table 1. The solid line shows a 1:1 ratio, the dashed lines show ratios of 2:1 and 1:2, and dot-dashed lines show ratios of 5:1 and 1:5.

assumptions regarding primary emissions and other factors that affect CN concentrations, CN10 values simulated on the basis of IMN agree reasonably well with observations (within a factor of 2 for most sites), while those based on CBHN, KBHN, and IIN underestimate the CN10 values by a factor of 2–10 for most sites. The CN10 values based on empirical formulas (EAN, EKN) are generally higher than observed ones (i.e., above 1:1 line) but are within a factor of  $\sim 2$  for most sites. IMN, EAN, and EKN overpredict CN10 by a factor of more than 2 for two, five, and nine sites, respectively. Although the annual mean nucleation rates predicted by different nucleation schemes differ by several orders of magnitude (Figure 3), the differences in the simulated CN10 are generally within one order of magnitude because of the emission of primary particles, coagulation, and transport. We would like to acknowledge that the present comparisons are subject to uncertainty associated with the parameterizations of primary particle emissions [e.g., Pierce and Adams, 2006] and interannual variations in the observed CN10 [e.g., Dal Maso et al., 2008]. While secondary particles dominate CN concentration in most parts of the troposphere, primary particles can contribute substantially to particle numbers near the source regions [Yu and Luo, 2009], and they can influence secondary particles formation via acting as condensation and coagulation sinks. Further measurements to characterize the size-resolved primary particle emissions are needed to reduce the uncertainty.

[16] The comparisons shown in Figures 5 and 6 are limited to 21 sites over the continents. Figure 5 also indicates large differences in the predicted particle number concentrations over oceans, especially between theoretical models (IMN, IIN, CBHN, and KBHN) and empirical for-

mulas (EAN and EKN). The ship-based data archived on the NOAA Pacific Marine Environmental Laboratory (PMEL) Atmospheric Chemistry Data Server provide an extensive set of aerosol number concentration data with large spatial coverage over the oceans and can be used to assess the modeled predictions. Figure 7 shows the total number concentrations of condensation nuclei larger than 4 nm (CN4) simulated with six different nucleation schemes. The symbols overlaid on each panel are the measured values from 13 ship-cruise campaigns taken by the PMEL atmospheric chemistry group (MAGE-92, RITS-93, RITS-94, ACE-1, ACE-2, INDOEX99, NAURU99, ACE-Asia, NEAQS-2002, NEAQS-2004, TexAQS-GoMACCS, ICEALOT, and VOCALS; see <http://saga.pmel.noaa.gov/data> for more information) and another ship cruise from the English Channel to the coast of Antarctica reported by Koponen et al. [2002]. It should be noted that the model results in Figure 7 represent annual mean values (for year 2006), while the observations for a given ship cruise represent average number concentrations of particles detected during a certain period of time in a specific month of a certain year. This kind of comparison (including the one discussed below for aircraft data) is necessary to establish the global 3-D pictures of particle number concentrations, and is justified by the relatively small seasonal and annual variations of total particle number concentrations over remote oceans and in the middle and upper troposphere. The number concentrations measured during some cruises are for particles larger than  $\sim 3$  nm while others are for particles larger than  $\sim 5$  nm. For comparison, the simulated results shown are for particles larger than 4 nm. The difference caused by different cut-off sizes is less than  $\sim 10$ –20%.

[17] The ship data show clearly that total aerosol number concentrations over the ocean are generally below  $1000 \text{ cm}^{-3}$  except near coastal regions. The EAN and EKN schemes overpredict the CN4 over tropical and subtropical oceans by a factor of up to  $\sim 10$ . Such a significant overprediction clearly indicates that the empirical formulas derived from the measurements taken in several land-based stations [Riipinen et al., 2007; Kuang et al., 2008] are likely to be invalid over the tropical and subtropical oceans. Under the present model assumptions regarding primary emissions and other factors that affect CN concentrations, the simulations based on the IMN scheme capture the observed CN4 gradients near the coast regions of Asia, India, Europe, and the eastern United States. The simulated CN4 over remote oceans based on the IMN scheme are generally within a factor of 2 when compared to ship data. The factors contributing to the difference at a specific location include the uncertainties in the model (emission, chemistry, microphysics, transport, and scavenging) and observations (counting efficiency for small particles, etc.), seasonal variations (annual mean versus daily mean), and spatial inhomogeneity (grid-box average versus value at a specific location). Overall, the IMN prediction agrees well with ship data. The low CN4 over remote oceans predicted by BHN and IIN schemes are generally consistent with the ship data, indicating that in situ nucleation is not necessary to explain the observed CN4 over remote oceans. Nevertheless, BHN and IIN significantly underpredict the CN4 near the coastal regions, associated with the underpredictions of nucleation and particles over major continents (Figures 5 and 6).



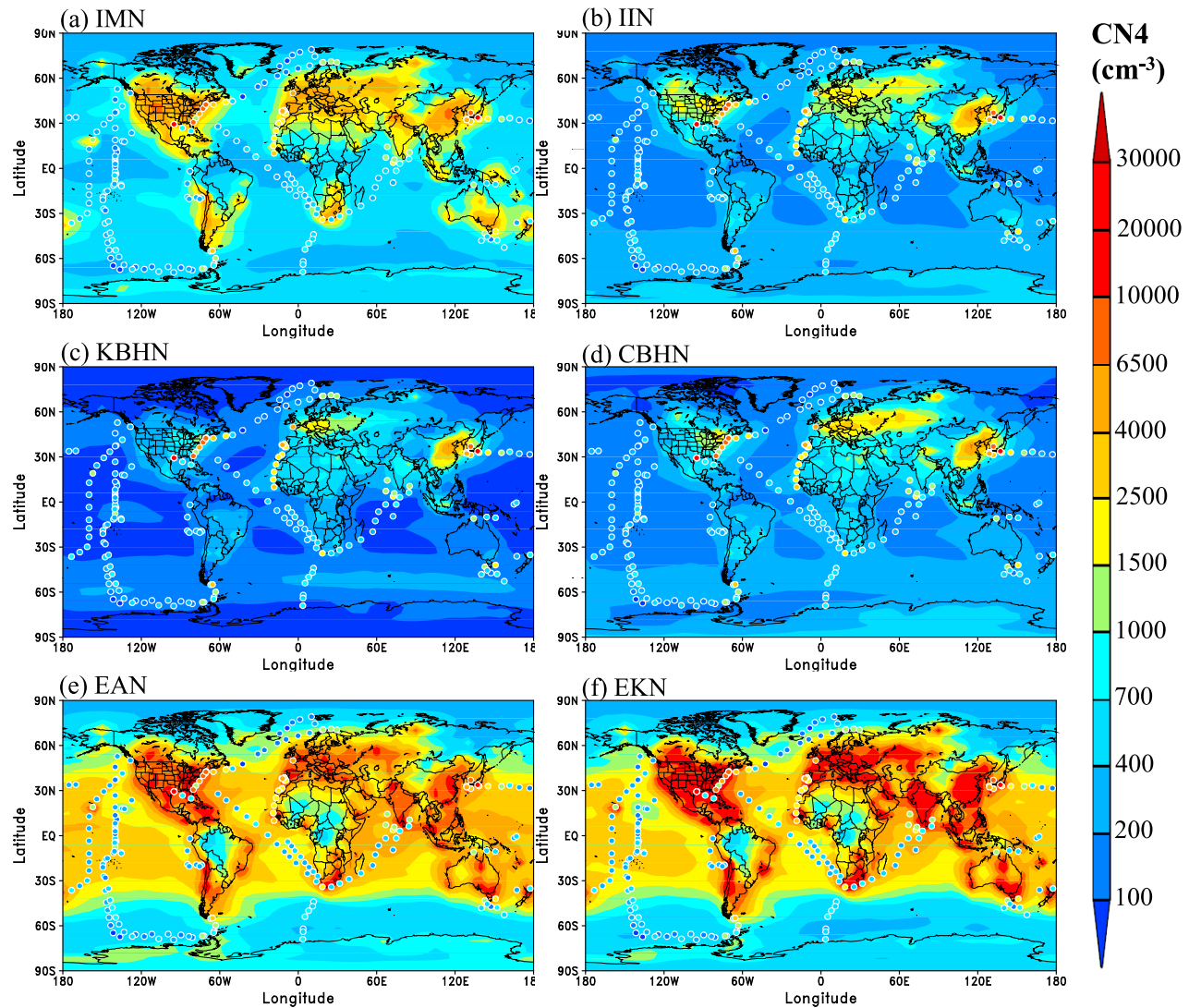


**Figure 7.** Horizontal spatial distributions of annual mean number concentrations of particles larger than 4 nm (CN4) in the lower boundary layer (0–0.4 km) simulated with six different nucleation schemes described in Table 1. Overlapped on the plots for comparison are ship-based measurements of CN4 during 13 ship-cruise campaigns taken by the PMEL Atmospheric chemistry group and another ship cruise from the English Channel to the coast of Antarctica reported by *Koponen et al.* [2002].

[18] So far, our comparisons with measurements have been limited to surface-based measurements of particle number concentrations in the lower boundary layer. To assess the vertical structure of global particle number concentrations, we use the total number concentrations of ultrafine condensation nuclei (UCN) measured with a CN counter (low cut-off size  $\sim 3\text{--}4$  nm, high cut-off size  $\sim 3000$  nm) during a number of aircraft-based field campaigns (GLOBE, ACE-1, PEM-Tropics A and B, TRACE-P, INTEX-A, NAMMA, TC-4, and ARCTAS). Information about these field measurements can be found in the work by *Clarke and Kapustin* [2002], NASA's Global Tropospheric Experiment (GTE) database Web site, and corresponding field campaign websites. Figure 8 gives 3-D and 2-D spatial distributions of the observed UCN concentrations. Figure 8a contains about 63,000 1-minute-average data points, plotted in the 3-D coordinate system based on the measurement

locations (longitude, latitude, and pressure or sigma). In Figure 8b, to avoid overlap owing to the large number of data points, the sigma-latitude cross section is divided into a  $0.01^\circ \times 1^\circ$  grid, wherein all data, at all longitudes, are averaged. The data shown in Figure 8, obtained during nine different airborne field campaigns, cover a wide range of areas and seasons. The high UCN regions in the tropical upper troposphere and northern midlatitude lower troposphere, and low UCN regions in the tropical lower troposphere and the Arctic, can be clearly seen from Figure 8. The large amount of UCN data given in Figure 8, along with a number of other airborne measurements reported in the literature [e.g., *Brock et al.*, 1995; *Heintzenberg et al.*, 2003; *Lee et al.*, 2003], consistently show that the average UCN concentration in the tropical upper troposphere is generally in the range of  $\sim 5000\text{--}10,000$   $\text{cm}^{-3}$  at standard temperature and pressure (STP). The UCN concentrations in the tropical

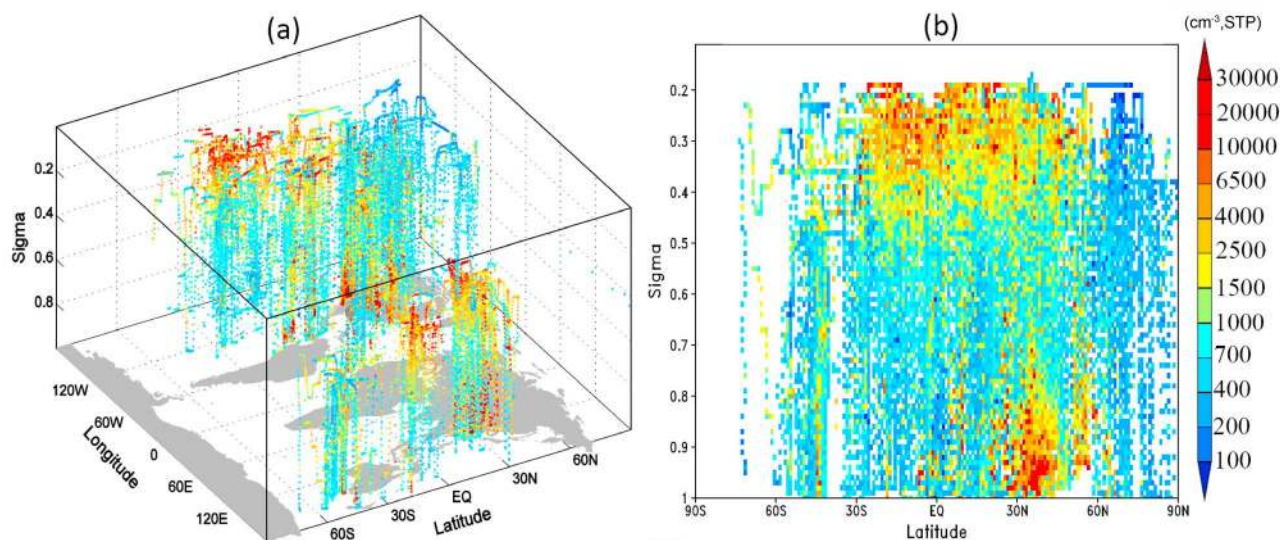


**Figure 8.** (a) Three-dimensional and (b) 2-D spatial distributions of ultrafine condensation nuclei (UCN) measured with CN counter (with low cut-off size of  $\sim 3\text{--}4$  nm) during a number of aircraft-based field campaigns (GLOBE, ACE-1, PEM-Tropics A and B, TRACE-P, INTEX-A, NAMMA, TC-4, and ARCTAS). Figure 8a contains about 63,000 1-minute-average data points. In Figure 8b, the sigma-latitude cross section is divided into  $0.01^\circ \times 1^\circ$  grids, wherein all data within a grid (at all longitudes) are averaged. The values have been normalized to standard temperature and pressure (STP, 1000 mbar and 298 K).

lower troposphere and the Arctic are generally below  $\sim 500\text{--}1000\text{ cm}^{-3}$  at STP.

[19] To compare the simulated UCN concentrations with aircraft-based measurements, we select modeling output data points at the locations (longitude, latitude, and altitude) corresponding to those observed. Figure 9 shows the 2-D distributions of these selected modeling data points (averaged in the same way as for the observed data shown in Figure 8b) based on six different nucleation schemes. Similar to Figure 7, the model results in Figure 9 represent annual mean values (for year 2006), while the observations in Figure 8 represent average number concentrations of particles detected during a certain period of time on a specific day of a year. The low cut-off size of CN counter is  $\sim 3$  nm in some measurements and is  $\sim 4$  nm in others. The simulated results are for all particles  $> 4$  nm. Both observed values in Figure 8 and modeled values in Figure 9 have been normalized to standard temperature and pressure (STP = 1000 mbar and 298 K).

[20] Figures 8 and 9 show that observed UCN concentrations have clear vertical structures and different nucleation schemes predict quite different vertical features of CN4. The CN4 values in the middle troposphere ( $\sim 500\text{--}600$  mbar) predicted by IMN are somehow higher than the observed ones, while those in the lower troposphere at latitudes of  $\sim 25^\circ\text{N}$  to  $50^\circ\text{N}$  are somehow lower than the observed values. The uncertainties in the model processes and observations, seasonal variations, and spatial inhomogeneity may all contribute to the difference. CBHN, KBHN, and IIN significantly underpredict UCN concentration in the lower troposphere (below  $\sim 500$  mbar). CN4 values based on CBHN are in reasonable agreement with observed values at higher altitudes ( $\sim 300\text{--}500$  mbar). However, CBHN over-

predict the particle number concentration in the upper troposphere ( $\sim 200$  mbar), likely as a result of the overprediction in the nucleation rates (Figure 4d) associated with the capillarity approximation implied in CBHN [Yu, 2007]. KBHN and IIN lead to the formation of new particles in the upper troposphere, but the predicted concentrations are smaller than IMN and are not able to account for the observed values. The overprediction of particle number concentrations over tropical oceans by EAN and EKN extends from the surface (also see Figures 7e and 7f) to around  $\sim 400$  mbar. All nucleation schemes predict relatively low CN4 values over the Arctic region, in agreement with the data.

[21] The IMN prediction captures the low CN concentrations over tropical oceans and the observed minimum particle number concentration in the middle troposphere over middle latitudes in the Northern Hemisphere. In agreement with observations, IMN predictions indicate two peak particle number concentration zones: one located in the boundary layer over continents at middle latitudes in the Northern Hemisphere and the other in the tropical upper troposphere. Such a two-peak distribution can also be seen from IIN, CBHN, and KBHN simulations. The zone in the boundary layer is a result of high anthropogenic sulfur emissions. In contrast, the zone in the tropical upper troposphere appears to be largely associated with naturally emitted sulfur species (DMS and oxidation products) and clean marine air lofted by convection and scavenged of most preexisting particles. The downward transport of particles formed aloft is a major source of sulfate particles in the tropical regions (especially over oceans), which can be seen clearly from the vertical profile of sulfate particle size distributions in the region [Yu and Luo, 2009]. The downward

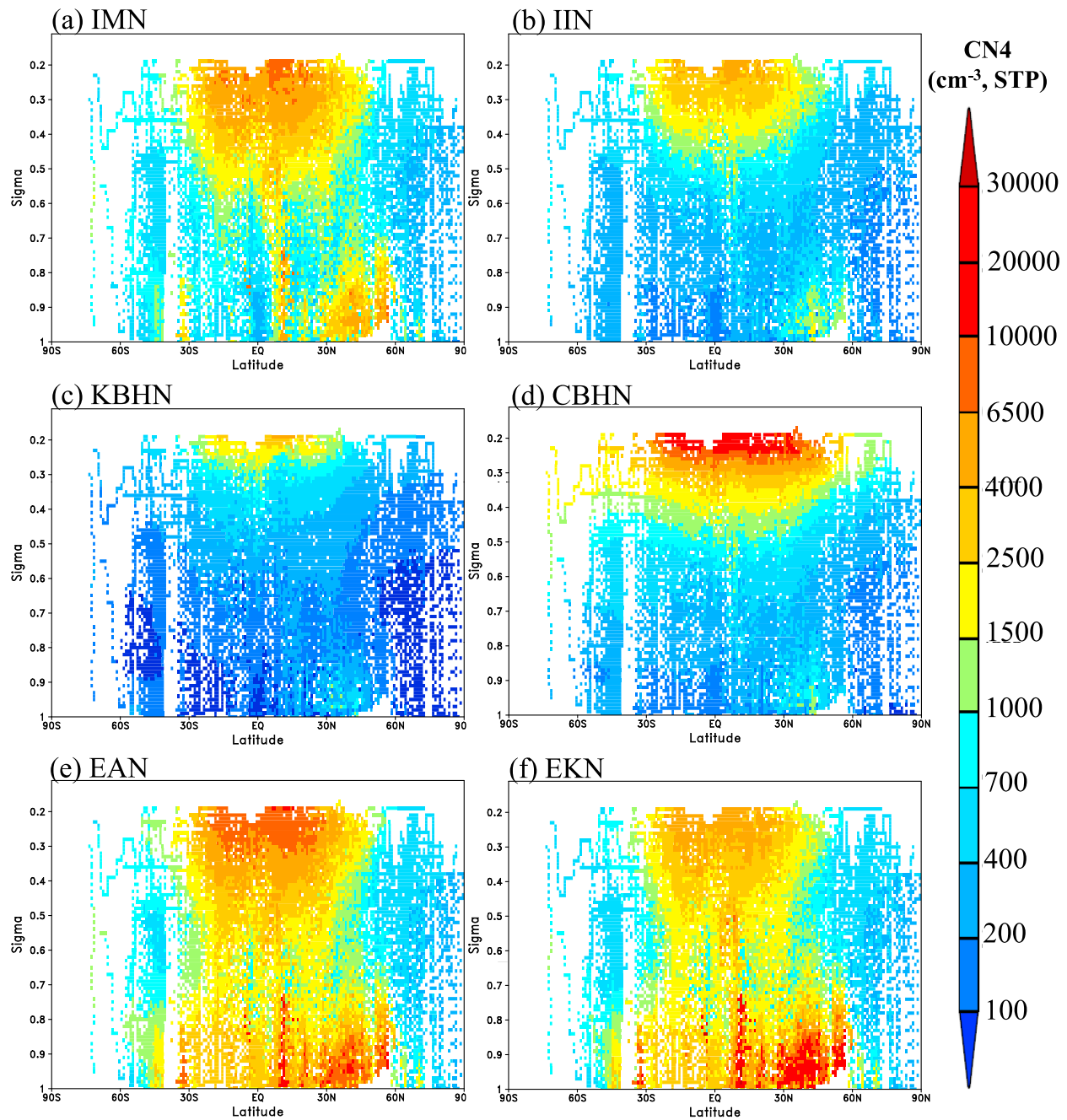


**Figure 9.** Two-dimensional distributions of these selected modeling data points (averaged in the same way as for the observed data shown in Figure 7b) based on six different nucleation schemes. The values have been normalized to standard temperature and pressure (STP, 1000 mbar and 298 K).

transport of particles in the tropical regions has been suggested in a number of previous studies [e.g., Raes, 1995; Clarke *et al.*, 1999a, 1999b], but these particles have generally been considered to nucleate via binary homogeneous nucleation. By comparing measured  $[\text{H}_2\text{SO}_4]$  with critical  $[\text{H}_2\text{SO}_4]$  required for a nucleation rate of  $1 \text{ cm}^{-3}\text{s}^{-1}$  (calculated with the parameterization of Wexler *et al.* [1994]), Clarke *et al.* [1999a, 1999b] suggested that the classical BHN theory of natural sources of sulfuric acid could account for the observed nucleation in the near-cloud

environment. The present study shows that the formation of these particles in the tropical upper troposphere, based on thermodynamically and kinetically most up-to-date ion and neutral nucleation mechanisms, appears to be dominated by ion nucleation instead of neutral nucleation (Figures 4 and 9). In a separate detailed study on the mechanism of particle production near marine clouds (manuscript in preparation), we show that the observed nucleation in the near-cloud environment is consistent with IMN mechanism while BHN (based on KBHN) is totally negligible. It appears that the

BHN rates based on the parameterization of *Wexler et al.* [1994] are even higher than those of CBHN [*Vehkamäki et al.*, 2002], which are known to have already over-predicted BHN rates by around three orders of magnitude [*Hanson and Lovejoy*, 2006; *Yu*, 2007].

## 5. Summary and Discussion

[22] The main objective of this study was to identify the nucleation scheme(s) that can account for both the absolute values and spatial distributions of particle number concentrations in the troposphere, through comparing global aerosol simulations based on six different nucleation schemes with an extensive set of land-, ship-, and aircraft-based particle number concentration measurements. The nucleation schemes considered in the present study included: ion-mediated nucleation (IMN) [*Yu and Turco*, 2000; *Yu*, 2010], ion-induced nucleation (IIN) [*Lovejoy et al.*, 2004; *Modgil et al.*, 2005], kinetic binary homogeneous nucleation (KBHN) [*Yu*, 2007, 2008], classical binary homogeneous nucleation (CBHN) [*Noppel et al.*, 2002; *Vehkamäki et al.*, 2002], empirical activation nucleation (EAN) and empirical kinetic nucleation (EKN) [*Riipinen et al.*, 2007; *Kuang et al.*, 2008].

[23] We showed that nucleation rates predicted on the basis of different schemes vary significantly both in absolute values and in their spatial distributions. The comparisons of simulated global particle number concentrations with land-, ship-, and aircraft-based measurements indicated that, under the present model assumptions regarding primary emissions and other factors that affect CN concentrations, only the IMN scheme could reasonably account for the absolute values (within a factor of  $\sim 2$ ) and spatial distributions of total particle number concentrations in the whole troposphere. The IMN prediction captured the low concentrations in the lower troposphere over tropical oceans and the observed minimum in particle number concentration in the middle troposphere over middle latitudes in the Northern Hemisphere. Consistent with observations, IMN simulations indicated two peak particle number concentration zones: one located in the boundary layer over continents at middle latitudes in the Northern Hemisphere because of high anthropogenic sulfur emissions, and the other in the tropical upper troposphere associated with naturally emitted sulfur species. The downward transport of particles formed in the upper troposphere is a major source of sulfate particles in the tropical regions. CBHN, KBHN, and IIN significantly underpredicted particle number concentration in the lower troposphere (below  $\sim 500$  mbar), especially in the boundary layer over major continents (by a factor of up to  $\sim 10$ ). In the upper troposphere, KBHN and IIN lead to the formation of new particles, but the predicted concentrations were much smaller than the observed values. In contrast, CBHN overpredicted the particle number concentration in the upper troposphere ( $\sim 200$  mbar). EAN and EKN significantly overpredicted the particle number concentrations over tropical and subtropical oceans (by a factor of up to  $\sim 10$  in the boundary layer), and such overpredictions extended from the ocean surface to around  $\sim 400$  mbar. It should be noted that the current EAN and EKN parameterizations assume constant prefactors and the performance of EAN and EKN parameterizations could be improved if the depen-

dence of prefactors on other parameters (such as temperature, etc.) can be identified and incorporated.

[24] Our results suggest that ion-mediated  $\text{H}_2\text{SO}_4\text{-H}_2\text{O}$  nucleation appears to dominate over neutral  $\text{H}_2\text{SO}_4\text{-H}_2\text{O}$  nucleation, not only in the lower troposphere but also in the middle and upper troposphere. According to the recently developed KBHN model constrained by multiple independent laboratory measurements,  $\text{H}_2\text{SO}_4\text{-H}_2\text{O}$  binary homogeneous nucleation is negligible when compared to IMN, even in the cold upper troposphere. Previous conclusions about the importance of BHN in the upper troposphere based on the CBHN model should be revisited, as the CBHN model has been shown recently in laboratory and theoretical studies to overpredict the nucleation rates under upper tropospheric conditions by three orders of magnitude. The present global scale study, combined with previous well-constrained case studies of nucleation events observed in boreal forests [*Yu and Turco*, 2008], and the fact that the IMN model is based on state-of-the-art thermodynamic and laboratory data [*Yu*, 2010], make a strong case for the importance of ion nucleation in the troposphere. This may have important implications because ion nucleation rates and hence global particle number abundance are subject to the influence of ionization rate variations associated with solar activities, which may amplify the impact of solar variations on Earth's climate. The magnitude of solar variations on the abundance of climate effective particles remains to be investigated. We would like to point out that there exists controversy over the importance of ion-mediated nucleation versus neutral nucleation based on the multiple-instrument characterization of nucleation events in boreal forests [*Laakso et al.*, 2007; *Kulmala et al.*, 2007; *Manninen et al.*, 2009; *Yu and Turco*, 2008; *Yu*, 2010]. The possible reasons for difference in the interpretation of the same measurements have been discussed in detail in *Yu* [2010]. It should also be noted that nucleation has been observed to be enhanced in recent laboratory studies when sulfuric acid is produced via  $\text{SO}_2 + \text{OH}$  reaction (rather than from liquid samples) [e.g., *Berndt et al.*, 2006; *Benson et al.*, 2008]. However, the level of enhancement differs significantly on the basis of the studies of the two different groups [*Du and Yu*, 2009] and a theory considering the enhancement remains to be developed. Some yet-to-be-identified nucleation mechanisms (both neutral and ion-mediated, involving species in addition to  $\text{H}_2\text{SO}_4$  and  $\text{H}_2\text{O}$ ) may occur in the atmosphere as well. Such new nucleation mechanisms, when available, should also be assessed against aerosol measurements with global coverage.

[25] As far as we know, this study represents the first comprehensive comparison of global particle number simulations with land-, ship-, and aircraft-based measurements, which establishes a global 3-D picture of particle number abundance in the troposphere. Nevertheless, some of these comparisons were between simulated annual mean values and short-term ship and aircraft measurements. The present global aerosol microphysical simulations are also subject to uncertainties associated with parameterizations of primary particles, contributions of secondary organic species to particle growth, and cloud-scavenging and transport processes. For example, *Pierce and Adams* [2006] showed that sea-salt particle concentrations simulated by different emission schemes differ substantially. Our analyses indicate

that the uncertainties in primary particle emission parameterizations do not affect the conclusions of this paper, mainly because of the dominance of total particle number concentrations by secondary particles in most part of the troposphere [Yu and Luo, 2009]. Currently, it is hard to evaluate how the uncertainties in the secondary organic condensation and subgrid cloud processing may affect the simulated particle number distributions, largely associated with the poor understanding of the formation and properties of secondary organics and low spatial resolution of global models. Comparison with simulated particle properties with various detailed aerosol measurements, such as the one presented in this study, provides a mean to evaluate the performance of models and identify areas for further improvement. Simulations with higher horizontal spatial resolution (for example, with nested domain) and more detailed comparisons with field measurements (for example, the diurnal and seasonal variations of particle size distribution evolutions) should be carried out to improve our understanding of key processes controlling particle properties in the atmosphere.

[26] **Acknowledgments.** This study is supported by the NSF under grant AGS-0942106 and by NASA under grant NNX08AK48G. S.W. acknowledges funding support from EPA grant R83428601. The GEOS-Chem model is managed by the Atmospheric Chemistry Modeling Group at Harvard University with support from the NASA Atmospheric Chemistry Modeling and Analysis Program.

## References

- Benson, D. R., L.-H. Young, F. R. Kameel, and S.-H. Lee (2008), Laboratory-measured nucleation rates of sulfuric acid and water binary homogeneous nucleation from the  $\text{SO}_2 + \text{OH}$  reaction, *Geophys. Res. Lett.*, **35**, L11801, doi:10.1029/2008GL033387.
- Berndt, T., O. Böge, and F. Stratmann (2006), Formation of atmospheric  $\text{H}_2\text{SO}_4/\text{H}_2\text{O}$  particles in the absence of organics: A laboratory study, *Geophys. Res. Lett.*, **33**, L15817, doi:10.1029/2006GL026660.
- Bauer, S. E., D. L. Wright, D. Koch, E. R. Lewis, R. McGraw, L.-S. Chang, S. E. Schwartz, and R. Ruedy (2008), MATRIX (Multiconfiguration Aerosol TRacker of mIXing state): An aerosol microphysical module for global atmospheric models, *Atmos. Chem. Phys.*, **8**, 6003–6035.
- Bey, I., D. J. Jacob, R. M. Yantosca, J. A. Logan, B. Field, A. M. Fiore, Q. Li, H. Liu, L. J. Mickley, and M. Schultz (2001), Global modeling of tropospheric chemistry with assimilated meteorology: Model description and evaluation, *J. Geophys. Res.*, **106**, 23,073–23,095, doi:10.1029/2001JD000807.
- Bond, T. C., E. Bhardwaj, R. Dong, R. Jogani, S. Jung, C. Roden, D. G. Streets, and N. M. Trautmann (2007), Historical emissions of black and organic carbon aerosol from energy-related combustion, 1850–2000, *Global Biogeochem. Cycles*, **21**, GB2018, doi:10.1029/2006GB002840.
- Brock, C. A., P. Hamill, J. C. Wilson, H. H. Jonsson, and K. R. Chan (1995), Particle formation in the upper tropical troposphere: A Source of nuclei for the stratospheric aerosol, *Science*, **270**, 1650–1653.
- Clarke, A. D., et al. (1998), Particle nucleation in the tropical boundary layer and its coupling to marine sulfur sources, *Science*, **282**, 89–92.
- Clarke, A., V. Kapustin, F. Eisele, R. Weber, and P. McMurry (1999a), Particle production near marine clouds: Sulfuric acid and predictions from classical binary nucleation, *Geophys. Res. Lett.*, **26**(16), 2425–2428.
- Clarke, A., F. Eisele, V. Kapustin, K. Moore, D. Tanner, L. Mauldin, M. Litichy, B. Lienert, M. Carroll, and G. Albercook (1999b), Nucleation in the equatorial free troposphere: Favorable environments during PEM-Tropics, *J. Geophys. Res.*, **104**(D5), 5735–5744.
- Clarke, A. D., and V. N. Kapustin (2002), A Pacific aerosol survey. Part 1: A decade of data on particle production, transport, evolution, and mixing in the troposphere, *J. Atmos. Sci.*, **59**, 363–382.
- Dal Maso, M., A. Hyvärinen, M. Komppula, P. Tunved, V.-M. Kerminen, H. Lihavainen, Y. Viisanen, H.-C. Hansson, and M. Kulmala (2008), Annual and interannual variation in boreal forest aerosol particle number and volume concentration and their connection to particle formation, *Tellus, Ser. B*, **60**(4), 495–508.
- Du, H., and F. Yu (2009), Kinetic modeling of nucleation experiments involving  $\text{SO}_2$  and OH: New insights into the underlying nucleation mechanisms, *Atmos. Chem. Phys.*, **9**, 7913–7922.
- Evans, M. J., and D. J. Jacob (2005), Impact of new laboratory studies of  $\text{N}_2\text{O}_5$  hydrolysis on global model budgets of tropospheric nitrogen oxides, ozone, and OH, *Geophys. Res. Lett.*, **32**, L09813, doi:10.1029/2005GL022469.
- Hanson, D. R., and E. R. Lovejoy (2006), Measurement of the thermodynamics of the hydrated dimer and trimer of sulfuric acid, *J. Phys. Chem. A*, **110**, 9525–9528, doi:10.1021/jp062844w.
- Heintzenberg, J., M. Hermann, and D. Theiss (2003), Out of Africa: High aerosol concentrations in the upper troposphere over Africa, *Atmos. Chem. Phys.*, **3**(4), 1191–1198.
- Kivekäs, N., et al. (2009), Long term particle size distribution measurements at Mount Waliguan, a high-altitude site in inland China, *Atmos. Chem. Phys.*, **9**, 5461–5474.
- Komppula, M., H. Lihavainen, A.-P. Hyvärinen, V.-M. Kerminen, T. S. Panwar, V. P. Sharma, and Y. Viisanen (2009), Physical properties of aerosol particles at a Himalayan background site in India, *J. Geophys. Res.*, **114**, D12202, doi:10.1029/2008JD011007.
- Koponen, I. K., A. Virkkula, R. Hillamo, V.-M. Kerminen, and M. Kulmala (2002), Number size distributions and concentrations of marine aerosols: Observations during a cruise between the English Channel and the coast of Antarctica, *J. Geophys. Res.*, **107**(D24), 4753, doi:10.1029/2002JD002533.
- Kuang, C., P. H. McMurry, A. V. McCormick, and F. L. Eisele (2008), Dependence of nucleation rates on sulfuric acid vapor concentration in diverse atmospheric locations, *J. Geophys. Res.*, **113**, D10209, doi:10.1029/2007JD009253.
- Kulmala, M., H. Vehkamäki, T. Petäjä, M. Dal Maso, A. Lauri, V.-M. Kerminen, W. Birmili, and P. McMurry (2004), Formation and growth rates of ultrafine atmospheric particles: A review of observations, *J. Aerosol Sci.*, **35**, 143–176.
- Kulmala, M., et al. (2007), Toward direct measurement of atmospheric nucleation, *Science*, **318**, 89–92, doi:10.1126/science.1144124.
- Laakso, L., S. Gagné, T. Petäjä, A. Hirsikko, P. P. Aalto, M. Kulmala, and V.-M. Kerminen (2007), Detecting charging state of ultra-fine particles: Instrumental development and ambient measurements, *Atmos. Chem. Phys.*, **7**, 1333–1345.
- Lee, S.-H., J. M. Reeves, J. C. Wilson, D. E. Hunton, A. A. Viggiano, T. M. Miller, J. O. Ballenthin, and L. R. Lait (2003), New particle formation by ion-induced nucleation in the upper troposphere and lower stratosphere, *Science*, **301**, 1886–1889.
- Liao, H., D. K. Henze, J. H. Seinfeld, S. Wu, and L. J. Mickley (2007), Biogenic secondary organic aerosol over the United States: Comparison of climatological simulations with observations, *J. Geophys. Res.*, **112**, D06201, doi:10.1029/2006JD007813.
- Lovejoy, E. R., J. Curtius, and K. D. Froyd (2004), Atmospheric ion-induced nucleation of sulfuric acid and water, *J. Geophys. Res.*, **109**, D08204, doi:10.1029/2003JD004460.
- Luo, G., and F. Yu (2010), A numerical evaluation of global oceanic emissions of alpha-pinene and isoprene, *Atmos. Chem. Phys.*, **10**, 2007–2015.
- Makkonen, R., et al. (2009), Sensitivity of aerosol concentrations and cloud properties to nucleation and secondary organic distribution in ECHAM5-HAM global circulation model, *Atmos. Chem. Phys.*, **9**, 1747–1766.
- Manninen, H. E., T. Nieminen, I. Riipinen, T. Yli-Juuti, S. Gagné, E. Asmi, P. P. Aalto, T. Petäjä, V.-M. Kerminen, and M. Kulmala (2009), Charged and total particle formation and growth rates during EUCAARI 2007 campaign in Hyytiälä, *Atmos. Chem. Phys. Discuss.*, **9**, 5119–5151.
- Martin, R. V., D. J. Jacob, R. M. Yantosca, M. Chin, and P. Ginoux (2003), Global and regional decreases in tropospheric oxidants from photochemical effects of aerosols, *J. Geophys. Res.*, **108**(D3), 4097, doi:10.1029/2002JD002622.
- Merikanto, J., I. Napari, H. Vehkamäki, T. Anttila, and M. Kulmala (2007), New parameterization of sulfuric acid-ammonia-water ternary nucleation rates at tropospheric conditions, *J. Geophys. Res.*, **112**, D15207, doi:10.1029/2006JD007977.
- Modgil, M. S., S. Kumar, S. N. Tripathi, and E. R. Lovejoy (2005), A parameterization of ion-induced nucleation of sulphuric acid and water for atmospheric conditions, *J. Geophys. Res.*, **110**, D19205, doi:10.1029/2004JD005475.
- Napari, I., M. Noppel, H. Vehkamäki, and M. Kulmala (2002), Parameterization of ternary nucleation rates for  $\text{H}_2\text{SO}_4\text{-NH}_3\text{-H}_2\text{O}$  vapors, *J. Geophys. Res.*, **107**(D19), 4381, doi:10.1029/2002JD002132.
- Nenes, A., S. N. Pandis, and C. Pilinis (1998), ISORROPIA: A new thermodynamic equilibrium model for multiphase multicomponent inorganic aerosols, *Aquat. Geochem.*, **4**, 123–152.
- Noppel, M., H. Vehkamäki, and M. Kulmala (2002), An improved model for hydrate formation in sulfuric acid–water nucleation, *J. Chem. Phys.*, **116**, 218–228.

- Oberdörster, G., Z. Sharp, V. Atudorei, A. Elder, R. Gelein, W. Kreyling, and C. Cox (2004), Translocation of inhaled ultrafine particles to the brain, *Inhal. Toxicol.*, *16*, 437–445.
- Park, R. J., D. J. Jacob, B. D. Field, R. M. Yantosca, and M. Chin (2004), Natural and transboundary pollution influences on sulfate-nitrate-ammonium aerosols in the United States: Implications for policy, *J. Geophys. Res.*, *109*, D15204, doi:10.1029/2003JD004473.
- Penttinen, P., K. L. Timonen, P. Tiittanen, A. Mirme, J. Ruuskanen, and J. Pekkanen (2001), Ultrafine particles in urban air and respiratory health among adult asthmatics, *Eur. Respir. J.*, *17*(3), 428–435.
- Pierce, J. R., and P. J. Adams (2006), Global evaluation of CCN formation by direct emission of sea salt and growth of ultrafine sea salt, *J. Geophys. Res.*, *111*, D06203, doi:10.1029/2005JD006186.
- Pierce, J. R., and P. J. Adams (2009), Uncertainty in global CCN concentrations from uncertain aerosol nucleation and primary emission rates, *Atmos. Chem. Phys.*, *9*, 1339–1356.
- Raes, F. (1995), Entrainment of free tropospheric aerosols as a regulating mechanism for cloud condensation nuclei in the remote marine boundary layer, *J. Geophys. Res.*, *100*(D2), 2893–2903.
- Ramanathan, V., P. J. Crutzen, J. T. Kiehl, and D. Rosenfeld (2001), Aerosols, climate, and the hydrological cycle, *Science*, *294*, 2119–2124, doi:10.1126/science.1064034.
- Reiter, R. (1992), *Phenomena in Atmospheric and Environmental Electricity*, 541 pp., Elsevier, New York.
- Riipinen, I., et al. (2007), Connections between atmospheric sulphuric acid and new particle formation during QUEST III–IV campaigns in Heidelberg and Hyytiälä, *Atmos. Chem. Phys.*, *7*, 1899–1914.
- Sorokin, A., F. Arnold, and D. Wiedner (2006), Formation and growth of sulfuric acid–water cluster ions: Experiments, modelling, and implications for ion-induced aerosol formation, *Atmos. Environ.*, *40*, 2030–2045.
- Spracklen, D. V., et al. (2008), Contribution of particle formation to global cloud condensation nuclei concentrations, *Geophys. Res. Lett.*, *35*, L06808, doi:10.1029/2007GL033038.
- Usoskin, I. G., and G. A. Kovaltsov (2006), Cosmic ray induced ionization in the atmosphere: Full modeling and practical applications, *J. Geophys. Res.*, *111*, D21206, doi:10.1029/2006JD007150.
- Vehkamäki, H., M. Kulmala, I. Napari, K. E. J. Lehtinen, C. Timmreck, M. Noppel, and A. Laaksonen (2002), An improved parameterization for sulfuric acid–water nucleation rates for tropospheric and stratospheric conditions, *J. Geophys. Res.*, *107*(D22), 4622, doi:10.1029/2002JD002184.
- Wang, M., and P. E. Penner (2009), Aerosol indirect forcing in a global model with particle nucleation, *Atmos. Chem. Phys.*, *9*, 239–260.
- Weber, R. J., J. J. Marti, P. H. McMurray, F. L. Eisele, D. J. Tanner, and A. Jefferson (1996), Measured atmospheric new particle formation rates: Implications for nucleation mechanisms, *Chem. Eng. Commun.*, *151*, 53–64.
- Wexler, A. S., F. W. Lurmann, and J. H. Seinfeld (1994), Modeling urban and regional aerosols—I. Model development, *Atmos. Environ.*, *28*, 531–546.
- Yu, F. (2006a), Effect of ammonia on new particle formation: A kinetic H<sub>2</sub>SO<sub>4</sub>–H<sub>2</sub>O–NH<sub>3</sub> nucleation model constrained by laboratory measurements, *J. Geophys. Res.*, *111*, D01204, doi:10.1029/2005JD005968.
- Yu, F. (2006b), From molecular clusters to nanoparticles: Second-generation ion-mediated nucleation model, *Atmos. Chem. Phys.*, *6*, 5193–5211.
- Yu, F. (2007), An improved quasi-unary nucleation model for binary H<sub>2</sub>SO<sub>4</sub>–H<sub>2</sub>O homogeneous nucleation, *J. Chem. Phys.*, *127*, 054301.
- Yu, F. (2008), Updated H<sub>2</sub>SO<sub>4</sub>–H<sub>2</sub>O binary homogeneous nucleation rate lookup tables, *J. Geophys. Res.*, *113*, D24201, doi:10.1029/2008JD010527.
- Yu, F. (2010), Ion-mediated nucleation in the atmosphere: Key controlling parameters, implications, and look-up table, *J. Geophys. Res.*, *115*, D03206, doi:10.1029/2009JD012630.
- Yu, F., and G. Luo (2009), Simulation of particle size distribution with a global aerosol model: Contribution of nucleation to aerosol and CCN number concentrations, *Atmos. Chem. Phys.*, *9*, 7691–7710.
- Yu, F., and R. P. Turco (2000), Ultrafine aerosol formation via ion-mediated nucleation, *Geophys. Res. Lett.*, *27*(6), 883–886, doi:10.1029/1999GL011151.
- Yu, F., and R. P. Turco (2008), Case studies of particle formation events observed in boreal forests: Implications for nucleation mechanisms, *Atmos. Chem. Phys.*, *8*, 6085–6102.
- Yu, F., Z. Wang, G. Luo, and R. P. Turco (2008), Ion-mediated nucleation as an important source of tropospheric aerosols, *Atmos. Chem. Phys.*, *8*, 2537–2554.
- Zhang, Q., et al. (2009), Asian emissions in 2006 for the NASA INTEX-B mission, *Atmos. Chem. Phys.*, *9*, 5131–5153.

B. Anderson, Chemistry and Dynamics Branch, Science Directorate, NASA Langley Research Center, Mail Stop 483, Hampton, VA 23681, USA.

T. S. Bates, Pacific Marine Environmental Laboratory, National Oceanic and Atmospheric Administration, 7600 Sand Point Way NE, Bldg. 3, Seattle, WA 98115, USA.

A. Clarke and V. Kapustin, Department of Oceanography, University of Hawai‘i at Mānoa, 1000 Pope Rd., MSB 506, Honolulu, HI 96822, USA.

G. Luo and F. Yu, Atmospheric Sciences Research Center, State University of New York at Albany, 251 Fuller Rd., Albany, NY 12203, USA. (yfq@asrc.cestm.albany.edu)

Y. Wang, Department of Environmental Science and Engineering, Tsinghua University, Rm 602, Beijing 100084, China.

S. Wu, Department of Geological and Mining Engineering and Sciences and Department of Civil and Environmental Engineering, Michigan Technological University, 1400 Townsend Dr., GMES/Dow 429, Houghton, MI 49931, USA.

R. M. Yantosca, School of Engineering and Applied Sciences, Harvard University, 29 Oxford St., Cambridge, MA 02138, USA.